

Band-offset non-commutativity of GaAs/AlGaAs interfaces probed by internal photoemission spectroscopy

Yan-Feng Lao, A. G. Unil Perera, Y. H. Zhang, and T. M. Wang

Citation: [Applied Physics Letters](#) **105**, 171603 (2014); doi: 10.1063/1.4901040

View online: <http://dx.doi.org/10.1063/1.4901040>

View Table of Contents: <http://scitation.aip.org/content/aip/journal/apl/105/17?ver=pdfcov>

Published by the [AIP Publishing](#)

Articles you may be interested in

[Polarization dependent photocurrent spectroscopy of single wurtzite GaAs/AlGaAs core-shell nanowires](#)

[Appl. Phys. Lett.](#) **102**, 142107 (2013); 10.1063/1.4801865

[Bandgap and band offsets determination of semiconductor heterostructures using three-terminal ballistic carrier spectroscopy](#)

[Appl. Phys. Lett.](#) **95**, 112102 (2009); 10.1063/1.3224914

[Synchrotron radiation photoemission spectroscopic study of band offsets and interface self-cleaning by atomic layer deposited Hf O 2 on In 0.53 Ga 0.47 As and In 0.52 Al 0.48 As](#)

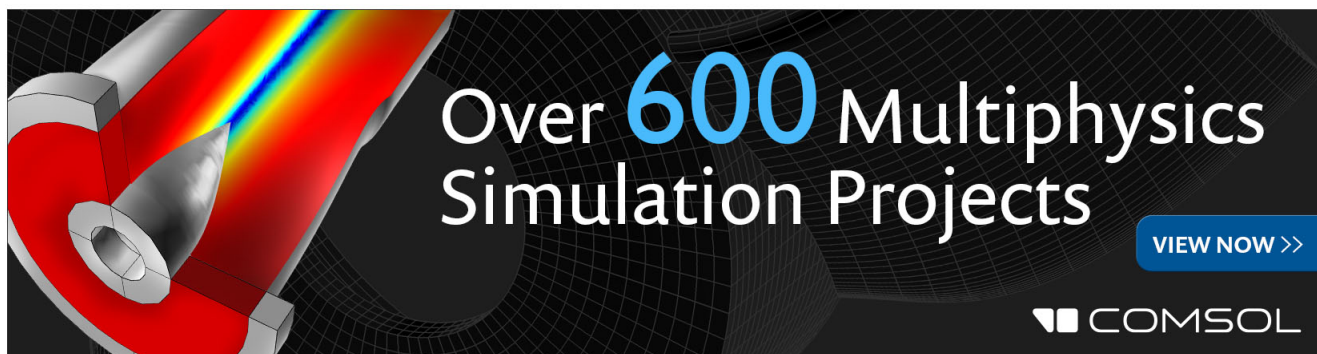
[Appl. Phys. Lett.](#) **93**, 182103 (2008); 10.1063/1.3020298

[Band offsets at the InAlGaAs/InAlAs \(001\) heterostructures lattice matched to an InP substrate](#)

[J. Appl. Phys.](#) **83**, 5852 (1998); 10.1063/1.367443

[Valence band discontinuity at a cubic GaN/GaAs heterojunction measured by synchrotron-radiation photoemission spectroscopy](#)

[Appl. Phys. Lett.](#) **70**, 2407 (1997); 10.1063/1.118886

The advertisement features a 3D cutaway illustration of a mechanical component with a red interior and a grey exterior. A rainbow-colored beam of light is shown passing through a hole in the component. The background is dark with a grid pattern. The text 'Over 600 Multiphysics Simulation Projects' is prominently displayed in white and blue. A blue button with the text 'VIEW NOW >>' is located in the bottom right corner. The COMSOL logo is in the bottom right corner.

Over **600** Multiphysics Simulation Projects

[VIEW NOW >>](#)

COMSOL

Band-offset non-commutativity of GaAs/AlGaAs interfaces probed by internal photoemission spectroscopy

Yan-Feng Lao,¹ A. G. Unil Perera,^{1,a)} Y. H. Zhang,² and T. M. Wang²

¹Department of Physics and Astronomy, Georgia State University, Atlanta, Georgia 30303, USA

²Key Laboratory of Artificial Structures and Quantum Control, Department of Physics and Astronomy, Shanghai Jiao Tong University, Shanghai 200240, China

(Received 1 August 2014; accepted 19 October 2014; published online 30 October 2014)

The GaAs/AlGaAs material system is believed to have a band offset without remarkable influence from the interface. We report here probing a slightly higher (5–10 meV) valence-band offset at the GaAs-on-Al_{0.57}Ga_{0.43}As interface compared to that of the Al_{0.57}Ga_{0.43}As-on-GaAs interface, by using internal photoemission spectroscopy. This indicates the non-commutativity of band offset for GaAs/AlGaAs, i.e., the dependence on the order of the growth of the layers. This result is consistently confirmed by observations at various experimental conditions including different applied biases and temperatures. © 2014 AIP Publishing LLC. [<http://dx.doi.org/10.1063/1.4901040>]

The GaAs/Al_xGa_{1-x}As heterojunction is one of the material systems that have received intensive attention over the years.¹ In general, the offset between the energy bands of lattice-matched GaAs and Al_xGa_{1-x}As is considered to be predictable according to the bulk properties of constituents GaAs and Al_xGa_{1-x}As,² on the basis of the principle, e.g., the Anderson's rule.³ A common practice is to use the model-solid theory,⁴ where energy band parameters of individual materials are set in an absolute energy scale. This means the commutativity and transitivity of band offset;⁵ that is, the offset is independent of the order of growth (commutativity)⁶ and growth direction,⁷ and offset values are self-consistent among different material systems (transitivity).⁵ However, contradiction was found in a few experiments as to the commutativity, in which non-equal valence-band offsets (VBOs) were confirmed, showing a dependence on the order of growth.^{8,9} A re-evaluation of this property will be a necessity, since, as a mature material system, the GaAs/Al_xGa_{1-x}As heterojunction has been widely used in various optoelectronic and electronic devices. The band offset is critically determinative for their characteristics.

For a device consisting of symmetrical configuration of semiconductor layers, the transport properties (e.g., current-voltage characteristic) are expected to be symmetrical if the band offset is commutative. However, this contrasts with experiments on the nominally symmetrical GaAs/AlGaAs samples which exhibit non-symmetrical transport of carriers⁹ and photovoltaic (PV) operation at zero applied bias.¹⁰ The later is advantageous in favoring the performance of PV detectors owing to negligible dark current and thus minimized device noise. This non-symmetrical behavior was explained by (i) the inequivalence of barriers above and below the detector absorber,¹¹ (ii) dopant segregation,¹⁰ and (iii) the inequivalence of the GaAs/AlGaAs interfaces according to the growth order due to the incorporation of interfacial defects.⁹

In this letter, the dependence of the band offset on the GaAs/AlGaAs interfaces is reinspected using internal-

photoemission (IPE) spectroscopy.¹² The non-commutativity of VBO is identified, with a slightly higher (5–10 meV) VBO at the GaAs-on-Al_{0.57}Ga_{0.43}As interface compared to that of the Al_{0.57}Ga_{0.43}As-on-GaAs interface. IPE is an attractive method for studying the properties of materials and optical processes occurring at the interface of two materials.^{12–15} IPE demonstrated advantages in characterizing new material systems including graphene and oxide-based structures,^{14,15} and it has also been adapted to characterize type-II InAs/GaSb superlattice photodetectors, confirming its unipolar operation,¹⁶ and the *n*-type Hg_{1-x}Cd_xTe/Hg_{1-y}Cd_yTe heterojunction.¹⁷

A single-period *p*-type GaAs/Al_{0.57}Ga_{0.43}As grown by a commercial manufacturer, IQE, is used in this study. A schematic of the structure is plotted in Fig. 1, consisting of three *p*-type GaAs regions, i.e., a top contact, a absorber (referred to as emitter), and a bottom contact. All of them are carbon doped to $1 \times 10^{19} \text{ cm}^{-3}$. The carbon doping has proven to have a good control in its spatial profile; for example, the delta doping control in the atomic scale has been observed by using scanning-tunneling microscopy.¹⁸ As such, dopant segregation is believed to be a trivial effect in our case. Also our IPE analysis does not show contradictory results which can be relevant to the dopant segregation.

The IPE refers to such a case where carriers are photo-excited and transmit from one material to another by passing through an interface. IPE is thus ideal for studying the interface properties. Upon photoexcitation in *p*-type GaAs layers, photoexcited holes move towards the GaAs-on-AlGaAs (or AlGaAs-on-GaAs) interface when a forward (reverse) bias is

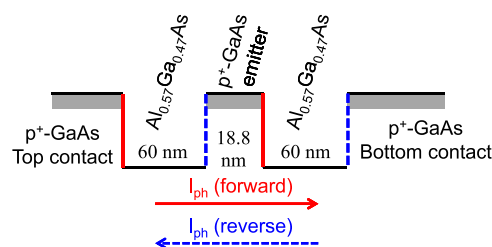


FIG. 1. Schematic of the *p*-type GaAs/Al_{0.57}Ga_{0.43}As structure used for studying the band offsets at the GaAs/AlGaAs interfaces.

^{a)}uperera@gsu.edu

applied (see Fig. 1). This allow for the characterization of the band offset of the corresponding interface through IPE fitting.^{12,16,17} The sample was processed by wet etching to produce square mesas, which was followed by evaporation of Ti/Pt/Au ohmic contacts onto the top and bottom *p*-type GaAs contact layers. A top ring contact with a window opened in the center was fabricated to allow front-side illumination. The experiments were carried out on $400 \times 400 \mu\text{m}^2$ mesas with an open area of $260 \times 260 \mu\text{m}^2$ in the center allowing for front-side illumination. A Perkin-Elmer system 2000 Fourier transform infrared spectrometer is used to measure the spectral response. A bolometer with known sensitivity is used for background measurements and calibration of the responsivity, in order to eliminate the influence of light source and optical components on the spectral line shape.

The IPE spectra are denoted by the quantum yield, Y , defined as the number of collected photocarriers per incident photon, which is proportional to the multiplication of spectral responsivity and photon energy.¹² Typical yield spectra are shown in Fig. 2(a) for 5.3 K, along with the spectra in the full spectral range shown in the inset. The primary contributions to the yield in *p*-type materials are due to hole transitions from the heavy-hole band to heavy-hole band and from the heavy-hole band to spin-orbit split-off band, which correspond to two IPE peaks at 0.2–0.35 eV and 0.35–0.65 eV, respectively. The low-energy cut-off (near-threshold regime) is due to the photoexcitation of photo-carriers in the *p*-type emitter, and their escape over the barrier, which are associated with the process across the VBO between the valence bands of the *p*-type GaAs and the AlGaAs barrier. The IPE process can be formulated in accordance with the processes of occurrence, allowing for fitting parameters with respect to the interface, using the method as described in Ref. 12.

The IPE fitting results for spectra under negative biases are shown in Fig. 2(b), which are in agreement with the near-threshold regimes. With the same fitting procedure applied to the spectra obtained at different biases and temperatures, the electric-field dependent thresholds at 5.3 K, 50 K, and 80 K are shown in Figs. 3(a), 3(b), and 3(c), respectively. The field-dependent behavior consists of three regions: I, II, and III as shown in Fig. 3. As the responding of the doped heterojunction to light relies on a photoemission mechanism,¹² the photoexcited holes from the emitter are in

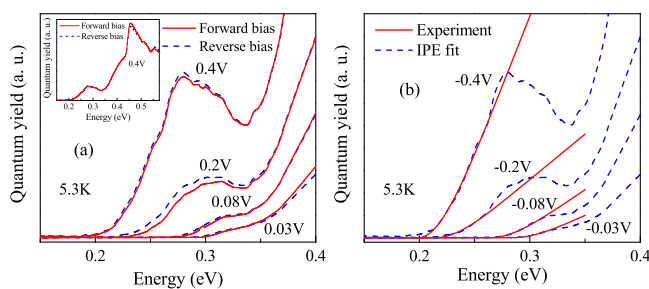


FIG. 2. (a) Representative IPE spectra at forward and reverse biases at 5.3 K, where the bias voltages of 0.03 V, 0.08 V, 0.2 V, and 0.4 V correspond to the electric field of 2.5 kV/cm, 6.7 kV/cm, 16 kV/cm, and 33.3 kV/cm. Inset is the overall quantum yield spectrum in the whole spectral range. (b) IPE fittings to the near-threshold quantum yield spectra at different reverse biases.

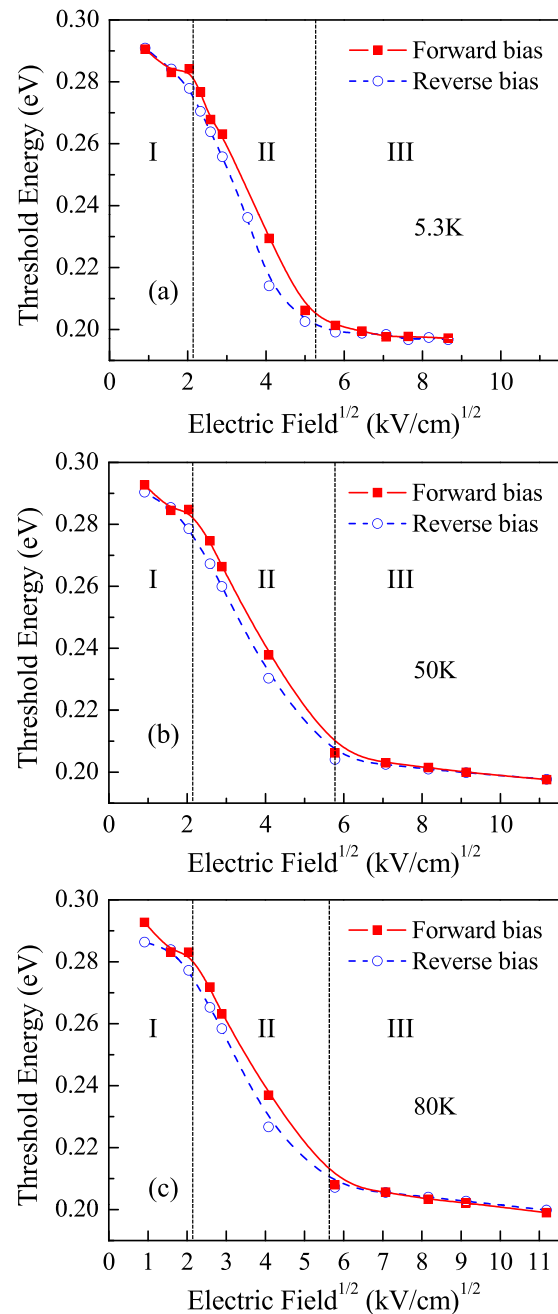


FIG. 3. (a) The IPE thresholds as a function of electric field at (a) 5.3 K, (b) 50 K, and (c) 80 K. The electric field range is divided into three regions. The photocurrent cancellation occurs in region I typically causing a zero-response point.¹⁹ The image-force caused barrier lowering dominates the region II, corresponding to the linear variation of threshold energy versus (electric field)^{1/2}. In the higher field region III, the hole tunneling through the barrier has the major influence on the threshold.

general able to emit towards both sides of the barriers. The ratio of the photoemission probability in one direction over another is strongly dependent on the difference between the heights of the barriers below and above the emitter, which in turn depends on the applied bias. For this reason, the response spectrum varies largely with the bias in the low-field region (I), associated with the photocurrent cancellation effect.¹⁹ At higher electric field, IPE in one direction dominates over the another. The IPE threshold is associated with the barrier height, and thus its variation is subject to the image-force caused barrier lowering¹² and the tunneling

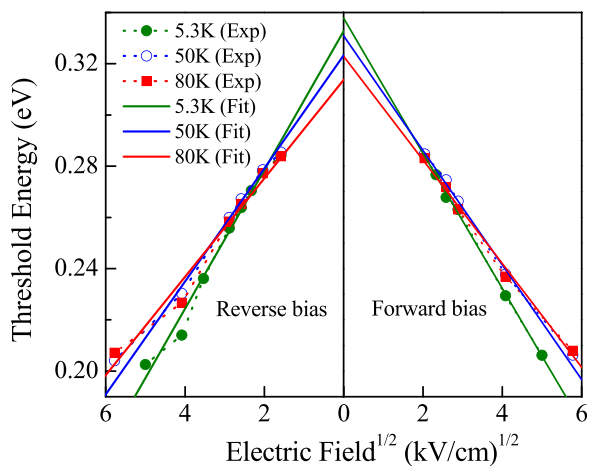


FIG. 4. The comparison of thresholds at different temperatures. The straight lines are fitting in the moderate electric field region (II as shown in Fig. 3) in order to extrapolate the thresholds at 0 V.

effect. As shown in Fig. 3, a linear variation of the IPE threshold versus (electric field)^{1/2} is found in the moderate electric-field region II, which is an indication of the dominant image-force caused lowering. Accordingly, a difference of the yield spectra between the forward and reverse biases can be identified, as shown in Fig. 2. In the even higher-field region III, hole tunneling dominates and has the remarkable influence on the threshold, which eliminates the difference in IPE thresholds at forward and reverse biases. To determine the thresholds, the data in the moderate field region where the threshold reduction can be explained by the image-force barrier lowering¹² should be used. This allows us to further correct the barrier lowering effect by extrapolating the threshold energy at 0 V, which is only associated with the GaAs/AlGaAs interface.

The threshold difference between the forward and reverse biases can be seen in the representative yield spectra at 0.08 V and 0.2 V, as shown in Fig. 2(a). Although the bottom contact is much thicker than the top contact, the contribution of absorption to the yield from top and bottom contact is nearly the same in according to the nearly overlapped yield spectra under forward and reverse biases of 0.4 V. This eliminates the effects due to layer absorption on probing a small threshold difference, which is thus considered as a cause due to the unequal GaAs-on-Al_{0.57}Ga_{0.43}As and Al_{0.57}Ga_{0.43}As-on-GaAs interfaces. To determine the difference quantitatively, the image-force caused barrier lowering is excluded by determining the threshold at 0 V, as shown in Fig. 4. This gives the threshold of the GaAs-on-Al_{0.57}Ga_{0.43}As interface 5–10 meV higher than that of the Al_{0.57}Ga_{0.43}As-on-GaAs interface. Although Yu *et al.*⁶ concluded the commutativity of the GaAs/AlAs band offset,

their results have an uncertainty of 70 meV, which is about an order of magnitude compared to our IPE results. Our conclusion regarding the greater band offset at the GaAs-on-Al_{0.57}Ga_{0.43}As interface is consistent with the previous reports by Tsai *et al.*⁹ on I-V characterization. They explained the results as being due to the incorporation of oxygen at the GaAs-on-AlGaAs interface.

To conclude, IPE studies on a single-emitter GaAs/Al_{0.57}Ga_{0.43}As structure are reported. Analysis shows a slight difference between the GaAs-on-Al_{0.57}Ga_{0.43}As and Al_{0.57}Ga_{0.43}As-on-GaAs interfaces, indicating the non-commutativity of GaAs/AlGaAs band offset. The resultant asymmetry favors applications such as photovoltaic operation at zero applied bias. For example, it can be used in a graded-barrier photovoltaic detector as demonstrated recently,¹⁹ to further improve the photovoltaic response.

This work was supported in part by the U.S. Army Research Office under Grant No. W911NF-12-2-0035 monitored by Dr. William W. Clark and in part by the U.S. National Science Foundation under Grant No. ECCS-1232184.

¹S. Adachi, *GaAs and Related Materials: Bulk Semiconducting and Superlattice Properties* (World Scientific, 1994).

²I. Vurgaftman and J. R. Meyer, *J. Appl. Phys.* **94**, 3675 (2003).

³R. L. Anderson, *IBM J. Res. Dev.* **4**, 283 (1960).

⁴C. G. Van de Walle and R. M. Martin, *Phys. Rev. B* **35**, 8154 (1987).

⁵A. D. Katnani and R. S. Bauer, *Phys. Rev. B* **33**, 1106 (1986).

⁶E. T. Yu, D. H. Chow, and T. C. McGill, *Phys. Rev. B* **38**, 12764 (1988).

⁷K. Hirakawa, Y. Hashimoto, and T. Ikoma, *Appl. Phys. Lett.* **57**, 2555 (1990).

⁸J. R. Waldrop, R. W. Grant, and E. A. Kraut, *J. Vac. Sci. Technol., B* **5**, 1209 (1987).

⁹K. L. Tsai, C. P. Lee, K. H. Chang, D. C. Liu, H. R. Chen, and J. S. Tsang, *Appl. Phys. Lett.* **64**, 2436 (1994).

¹⁰E. Luna, A. Trampert, A. Guzman, and E. Calleja, *J. Appl. Phys.* **98**, 044510 (2005).

¹¹H. Schneider, F. Fuchs, B. Dischler, J. D. Ralston, and P. Koidl, *Appl. Phys. Lett.* **58**, 2234 (1991).

¹²Y.-F. Lao and A. G. U. Perera, *Phys. Rev. B* **86**, 195315 (2012).

¹³V. Afanas'ev, *Internal Photoemission Spectroscopy: Principles and Applications* (Elsevier Science, 2010).

¹⁴R. Yan, Q. Zhang, W. Li, I. Calizo, T. Shen, C. A. Richter, A. R. Hight-Walker, X. Liang, A. Seabaugh, D. Jena, H. G. Xing, D. J. Gundlach, and N. V. Nguyen, *Appl. Phys. Lett.* **101**, 022105 (2012).

¹⁵Y. Hikita, M. Kawamura, C. Bell, and H. Y. Hwang, *Appl. Phys. Lett.* **98**, 192103 (2011).

¹⁶Y.-F. Lao, P. K. D. D. P. Pitigala, A. G. Unil Perera, E. Plis, S. S. Krishna, and P. S. Wijewarnasuriya, *Appl. Phys. Lett.* **103**, 181110 (2013).

¹⁷Y.-F. Lao, A. G. Unil Perera, and P. S. Wijewarnasuriya, *Appl. Phys. Lett.* **104**, 131106 (2014).

¹⁸L. Winking, M. Wenderoth, T. C. G. Reusch, R. G. Ulbrich, P.-J. Wilbrandt, R. Kirchheim, S. Malzer, and G. Dohler, *J. Vac. Sci. Technol., B* **23**, 267 (2005).

¹⁹Y.-F. Lao, P. K. D. D. P. Pitigala, A. G. Unil Perera, L. H. Li, S. P. Khanna, and E. H. Linfield, *Appl. Phys. Lett.* **104**, 131101 (2014).